Journal of Magnetic Resonance 278 (2017) 96–103

Contents lists available at ScienceDirect

Journal of Magnetic Resonance

journal homepage: www.elsevier.com/locate/jmr

Weak coupling between magnetically inequivalent spins: The deceptively simple, complicated spectrum of a ^{13}C-labeled trimethylated amine

Ulric B. le Paige [a,1], Bauke Smits [a,1], Peter 't Hart [b], Fons Lefeber [c], Nathaniel I. Martin [b], Hugo van Ingen [a,*]

[a] Macromolecular Biochemistry, Leiden Institute of Chemistry, Leiden University, The Netherlands
[b] Department of Chemical Biology & Drug Discovery, Utrecht Institute for Pharmaceutical Sciences, University Utrecht, The Netherlands
[c] NMR Facility, Leiden Institute of Chemistry, Leiden University, The Netherlands

ARTICLE INFO

Article history:
Received 28 February 2017
Revised 23 March 2017
Accepted 25 March 2017
Available online 27 March 2017

Keywords:
Magnetic equivalence
Sub-spectral analysis
Composite particle analysis
Trimethylated amine
J-coupling
$^4J_{HH}$

ABSTRACT

Magnetic inequivalence of nuclear spins is well known to cause additional splittings that complicate spectral analysis. Here, we present an extraordinary case of magnetic inequivalence, manifested in the 13-spin system of a ^{13}C,^{15}N-labeled trimethylated amine. All methyl group protons are chemically equivalent due to the molecular symmetry, but not all are magnetically equivalent as they have different $^1J_{CH}$ and $^3J_{CH}$ couplings. In general, spectra of such a large spin system can be expected to be extremely complicated by the presence of hundreds if not thousands of extra lines, caused by the strong coupling between inequivalent nuclei. Surprisingly, the ^{1}H spectrum presented consists of very few lines, in a pattern of the utmost simplicity. Using sub-spectral analysis we show that this is due to weak coupling between the magnetically inequivalent nuclei, as a consequence of the particular combination of coupling constants. We find that the $^4J_{HH}$ geminal methyl coupling constant is 0.43 Hz and $^2J_{CC}$ is ~0 Hz. In addition, we demonstrate that homo-decoupling can be used to transform the spin system to a set of fully equivalent spins, resulting in disappearance of $^4J_{HH}$-splittings. We believe this curious case is a highly instructive example of magnetic inequivalence. The spectra may be considered deceptively simple, as fewer lines are observed than one would anticipate. At the same time, the spectra are deceptively complicated, as they can very well be approximated by intuitive reasoning.

1. Introduction

Scalar coupling between nuclear spins is one of the defining features of solution NMR. It is used as a rich source of information on molecular structure [1], and encountered in the everyday practice of spectroscopists through the fine structure of resonance lines. The exact shape of the multiplet pattern that is generated by scalar coupling depends critically on the ratio of the frequency separation between the two nuclei, $\Delta\nu$, and their coupling constant, J. In the weak coupling regime ($\Delta\nu \gg J$) simple rules can predict the observed multiplet patterns. Spins that are strongly coupled ($\Delta\nu \lesssim J$) give rise to more complicated multiplets: the intensity of individual components depends strongly on $\Delta\nu/J$, and in larger spin systems additional, so-called combination lines may be observed. At the extreme end of strong coupling is the coupling between spins with identical chemical shifts ($\Delta\nu = 0$). In this case, the spins are either magnetically equivalent, when they have identical coupling constants to all other (non-equivalent) spins in the molecule, or magnetically *in*equivalent, when this is not the case [2]. The coupling between magnetically equivalent spins is inconsequential, as it cannot be observed. On the contrary, the coupling between magnetically inequivalent spins is observable and responsible for additional line splitting, a fact well established since the pioneering work of McConnell, McLean and Reilly [3]. The theory of magnetically inequivalent spin systems and analysis of their spectra has been thoroughly described in the 50s and 60s of last century [4–10]. These and other analyses show that, in particular for large spin systems, the strong coupling between magnetically inequivalent nuclei can generate so many additional splittings and additional lines that the extraction of accurate spin frequencies and scalar coupling constants is severely challenged [11–13].

Here, we revisit the analysis of magnetically inequivalent spin systems to describe an exceptional scenario where this spectral complexity is lost and a simple, essentially weakly coupled spectrum is obtained. We demonstrate this effect experimentally in a 13-spin system, a ^{13}C,^{15}N-labeled trimethylated amine, in which

* Corresponding author at: Einsteinweg 55, 2333 CC Leiden, The Netherlands.
E-mail address: h.van.ingen@lic.leidenuniv.nl (H. van Ingen).
[1] These authors have contributed equally.

http://dx.doi.org/10.1016/j.jmr.2017.03.016
1090-7807/

the three methyl groups are magnetically inequivalent. We show that the combination of large and small coupling constants in this spin system results in a system that can very well be treated as weakly coupled magnetically inequivalent spin pairs. We further demonstrate that the effects from magnetically inequivalence can be completely removed in this case by ^{13}C-spin state selective proton homo-decoupling. The curious spectrum of this compound and the controlled transformation to magnetic equivalence highlight the richness of scalar coupling phenomena in NMR.

2. Materials and methods

2.1. Synthesis

Compound **1**, systematic name 2-bromo-N,N,N-tri(methyl-^{13}C) ethan-1-aminium-1,1,2,2-d$_4$-N-^{15}N-chloride, was synthesized in a straightforward manner from fully isotope labeled trimethylammonium chloride and fully deuterated 1,2 dibromo-ethane (see Scheme 1). In a 10 ml round-bottom flask, tri(methyl-^{13}C)-ammonium-^{15}N chloride (100 mg, 1.05 mmol) was mixed with a 10-fold excess of 1,2-dibromoethane-1,1,2,2-d_4 (1.98 g, 0.91 ml, 10.5 mmol). DIPEA (365 μl, 2.1 mmol) was then added and the mixture was stirred for 15 min. A few drops of MeOH were added to ensure complete dissolution. The mixture was placed under an N_2 atmosphere and stirred for 96 h at 30 °C. The excess 1,2-dibromoethane-d_4 was removed by rotary evaporation and the residue suspended in cold EtOAc. After filtration, the solids were washed with cold EtOAc and dried under high vacuum. The yield was 413 mg of compound/DIPEA-HBr (94%). The resulting compound was characterized by HRMS ESI-TOF and NMR. *m/z*: expected mass for $C_2{}^{13}C_3H_9D_4Br^{15}N$ ([M]$^+$): 174.0548, experimentally obtained 174.0522 Da, and NMR (Fig. S1).

2.2. NMR spectroscopy

NMR spectra of compound **1** (~20 mM) in 100% D_2O were obtained at 298 K on a Bruker Avance III HD spectrometer operating at 600 MHz ^{1}H Larmor frequency and equipped with a cryoprobe. All 1D ^{1}H spectra were acquired in a single scan and zero-filled two times before Fourier transformation. Highest resolution spectra were obtained with 8 s. acquisition time and Lorentz-to-Gauss apodization with negative exponential broadening −1 Hz and the center of the Gaussian placed at 30% of the FID. Other spectra, including ^{15}N/^{13}C decoupled spectra, were recorded with 5 s acquisition time and apodized with −0.8 Hz negative exponential broadening and the center of the Gaussian shifted to 40% of the length of the FID. In order to obtain a high-resolution ^{15}N/^{13}C-decoupled 1D, a low power on-resonance WALTZ16-decoupling field was used: 260 Hz γB_2 at 49.9 ppm for ^{15}N, and 640 Hz γB_2 at 53.0 ppm for ^{13}C. The ^{15}N and ^{13}C chemical shifts were obtained from 2D H(C)N and 2D HMQC spectra. The homo-decoupled spectrum was recorded using the zghd.2 pulse program with continuous wave irradiation (~70 Hz γB_2) centered on the upfield $^1J_{CH}$ doublet component and 5 s acquisition time.

2.3. Simulations

There are several powerful programs that can simulate solution-state NMR spectra, e.g. [14–16]. We preferred to write our own simulation script as part of our learning process and to be able to tailor the simulations to our needs and requirements. Spectra of various AX-type spin systems were simulated using an in-house written GNU Octave [17] script that implements the composite particle approach (CPA) [18,19], as outlined by Diehl and coworkers [10]. Briefly, magnetically equivalent spins are grouped into a single composite particle, with total spin F_{max} equal to the sum of the grouped spins, e.g. $F_{max} = 3/2$ for three equivalent methyl protons. This particle can exist in independent spin states with a maximum spin F equal to F_{max}, $F_{max} - 1, \ldots$; e.g. for a system of one methyl group the allowed spin states are quartet ($F = 3/2$, Q) and doublet ($F = 1/2$, D), such that a trimethyl group can exist in any of 8 states such as QQQ, QQD, QDQ, *etc*. To solve the A-spin (^{1}H) spectrum, the Hamiltonian is factorized according to the total spin of the system m_T, the spin state of each particle, and the total spin $m_{T,X}$ of the X-nuclei (^{13}C). This procedure breaks down the 4096 × 4096 matrix for the 12-spin case into much smaller matrices of at most 36 × 36. The transition frequencies and intensities are then calculated using standard approaches. Each subspectrum is multiplied with a statistical weight to account for the degeneracy of the involved spin states. Lines corresponding to transitions with extremely low probability (intensity lower than $1{\cdot}10^{-4}$, whereas the largest peak has intensity 36) are omitted to ensure efficient drawing of the spectrum. For all remaining transitions an FID is simulated, these are subsequently added, an exponential decay to match the experimental lineshape is added, and the final FID is processed according to the experimental settings to yield the final spectrum.

In the weak-coupling approximation, the experimental spectrum was simulated by calculating FIDs according to the experimental settings for the outer, center and inner lines individually. For all three signals a weak $^2J_{NH}$ coupling was added. The effect of inequivalence was simulated by adding a weak $^4J_{HH}$ coupling to either 0, 3, or 6 equivalent protons for the outer, center and inner line, respectively. An exponential decay was added to match the experimental lineshape. Processing was identical to the experimental situation. All simulation scripts are available upon request.

3. Theory

In this section, we will, after a brief introduction, use the subspectral analysis approach to derive the boundary conditions that result in weakly coupled spectra of magnetically inequivalent spins.

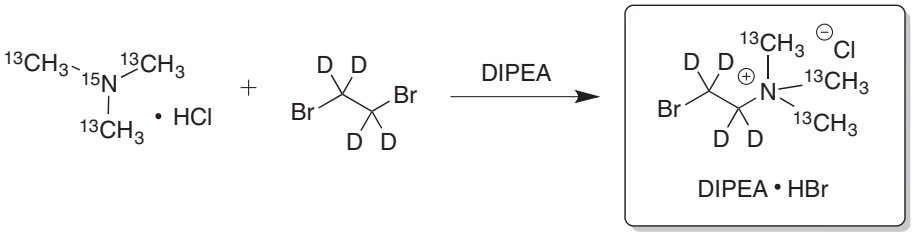

Scheme 1. Synthesis of compound **1**.

3.1. Sub-spectral analysis

The sub-spectral analysis framework was developed by Diehl, Bernstein and co-workers to ease the accurate determination of *J*-coupling values and chemical shifts in magnetically inequivalent systems [8,10]. The basic principle of this approach is to decompose the spectrum into much simpler sub-spectra, each with well-defined (apparent) chemical shifts and coupling constants. This decomposition reflects the factorization of the Hamiltonian, or equivalently the energy level diagram, into independent parts. Considering the A-spin spectrum of AX-type spin systems, the energy level diagram can be factorized based on the total magnetic quantum number $m_{T,X}$ for the X-spins: transitions of spin A are only allowed between wave functions that have $\Delta m_{T,X} = 0$ (the so-called X-approximation), in addition to the usual $\Delta m = \pm 1$ selection rule. Further factorization can be obtained by using wave functions that are constructed using the molecular symmetry, since selection rules only allow transitions between states of the same symmetry class [4]. Thus, the sub-spectra in the A-spectrum correspond each to a *sub*-energy level diagram formed by wave functions of one particular $m_{T,X}$ value and one particular symmetry class.

3.2. Conditions for weakly coupled sub-spectra

To explain how weakly coupled sub-spectra can arise, we turn to the textbook case of a 4-spin system with two pairs of magnetically inequivalent spins [3,5,20,21]. This spin system is labeled AA′XX′ in the extended notation of Pople [22,23], or $[AX]_2$ in the notation of Haigh [24]. The spin system is schematically illustrated in Fig. 1A together with definition of the coupling constants. The spectrum of the inequivalent A/A′ spins consists of eight lines, decomposed into two a_2 and two *ab* sub-spectra (sub-spectra are denoted in lowercase italics) (Fig. 1B). The two a_2 sub-spectra originate from sub-energy level diagrams that have the same functional shape as that for two equivalent spins, hence the a_2-designation. These corresponds to $m_{T,X} + 1$, i.e. X-spins in the αα-state, and to $m_{T,X} - 1$, i.e. X-spins in the ββ-state. In both subspaces, the A/A′-spins are described by fully equivalent, virtual *a*-spins with frequency $\nu_a = \nu_A \pm |J_{AX} + J_{AX'}|$. Their equivalence may be intuitively understood by imagining a molecule with the X/X′-spins both in the α or both in the β-spin state: the A/A′-spins are indistinguishable due to the twofold symmetry of the molecule. This is not true for mixed α/β-states; hence the A/A′-spins in the $m_{T,X} = 0$ space are magnetically *in*equivalent and subject to J_{AA}/J_{XX}-coupling. In this subspace, the A/A′-spins form a strongly coupled *ab*-type spin system, with frequency difference $\Delta\nu_{ab} = |J_{AX} - J_{AX'}|$ and *J*-coupling $J_{ab} = |J_{AA'}| \pm |J_{XX'}|$ between the virtual *a* and *b*-spins. Since this space is formed by both symmetrical and antisymmetrical wave functions there are two *ab*-sub-spectra. An explicit presentation of the wave functions and energy diagram of the AA′XX′-system, based primarily on the analysis by Flynn et al. [20], is presented in Fig. S2.

We will now set two boundary conditions that will result in a dramatic simplification of the spectrum. First, either J_{XX} or J_{AA} is near zero. In this case the two *ab*-sub-spectra in Fig. 1B have the same effective splitting and collapse into a single *ab*-sub-spectrum, as shown in Fig. 1C. Second, the frequency separation between the virtual *a* and *b*-spins $\Delta\nu_{ab}$ is much larger than their effective coupling constant J_{ab}, i.e. when $J_{XX} \sim 0$:

$$|J_{AX} - J_{AX'}| \gg |J_{AA'}| \tag{1}$$

Because the *a*,*b*-spins are now no longer strongly coupled, we redefine them as weakly coupled *a*,*x*-spins. The $m_{T,X} = 0$ sub-spectrum is a symmetric doublet, split by J_{AA}, and is best labeled as an *ax*-sub-spectrum (Fig. 1D). Thus, under the above two conditions the spectrum of 8 lines and 5 different intensity levels of Fig. 1A is reduced to 6 lines with only 2 different intensities, the

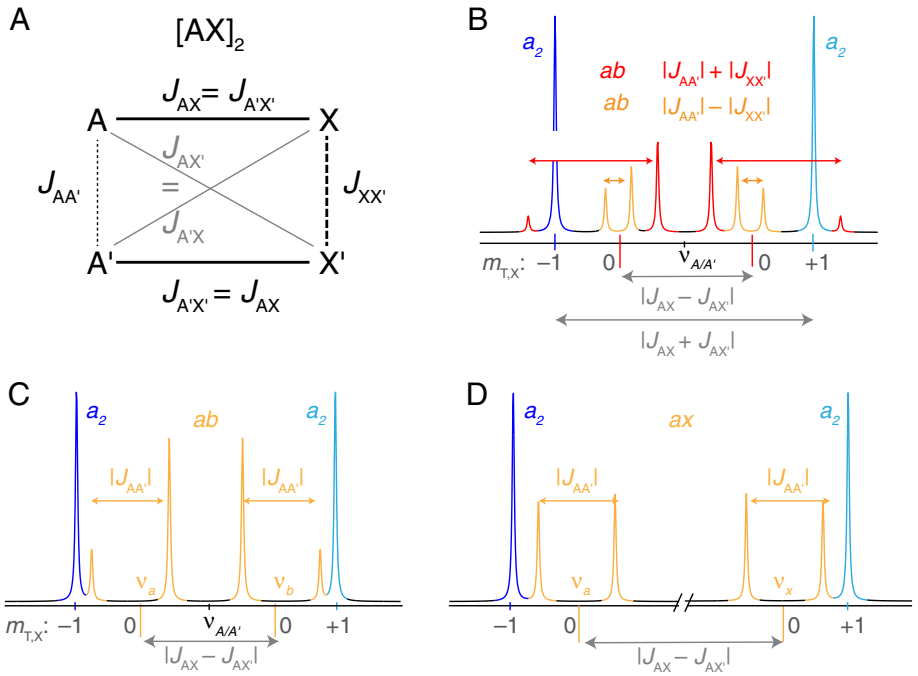

Fig. 1. Sub-spectral analysis of the $[AX]_2$ spin system illustrating the spectral simplification when J_{XX} couplings are negligible and J_{AX} couplings are large. (A) Spin topology of the $[AX]_2$ spin system with all *J*-couplings indicated (B,C,D) Simulated spectra of the AA′-part of the AA′XX′ spectrum using the following parameters: $J_{AX} = 7.5$, $J_{AX'} = 2.5$, $J_{AA'} = 3$, and $J_{XX'} = 2$ Hz in (B); $J_{XX'} = 0$ Hz in (C) and in (D) $J_{XX'} = 0$ Hz and $J_{AX} = 150$ Hz. Decomposition of the spectrum into sub-spectra is indicated (a_2 in blue/cyan; *ab* in red/orange). Effective Larmor frequency differences and coupling constants between the *a*,*b*(*x*) spins in the *ab*(*x*)-sub-spectra are indicated. The total spin state of the X-spins, $m_{T,X}$ is indicated as −1, 0 or +1. (For interpretation of the references to color in this figure legend, the reader is referred to the web version of this article.)

sum of two a_2 and two overlapping *ax*-sub-spectra in Fig. 1D. This dramatic simplification may arise if J_{AX} is very large compared to the other coupling constants.

3.3. Extension to $[AX]_3$ and $[A_3X]_3$ spin systems

The simplified pattern of Fig. 1D in the $[AX]_2$ spin system can be extended to more complicated AX-type spin systems in a predictable manner. As an intermediate step towards the $[A_3X]_3$ system, it is useful to consider the A-spin spectrum in the 6-spin system $[AX]_3$, first described by Jones et al. [9]. In general, this spectrum consists of 56 transitions that can be grouped in six sub-spectra of three virtual spins: two a_3-patterns for $m_{T,X} = \pm^3/_2$, i.e. where the X-spins are in the ααα/βββ-spin state, two ab_2- and two *abc*-patterns for $m_{T,X} = \pm^1/_2$. In the special case where $J_{XX} = 0$, it can be shown that the *abc*-pattern is reduced to another ab_2-pattern [9], a situation depicted in Fig. 2A. The frequency difference between the virtual *a* and *b* spin is $|J_{AX} - J_{AX'}|$, with apparent coupling constant J_{AA} (when $J_{XX} = 0$). Here, we label the $m_{T,X} = \pm^1/_2$ sub-spectra on one side of A-multiplet as ab_2 and as a_2b on the other side, reflecting the different orientations of the ab_2-pattern. This complicated multiplet is again dramatically simplified when $|J_{AX} - J_{AX'}| \gg |J_{AA}|$, as shown in Fig. 2B. Under these conditions, the *a* and *b* spins are effectively weakly coupled and the sub-spectra reduce to a_2x and ax_2-patterns. The logical progression from a_3 to a_2x and ax_2 can also be appreciated considering the X spin states: from ααα ($m_{T,X} = +^3/_2$, a_3) to states of the ααβ ($m_{T,X} = +^1/_2$, a_2x) to αββ-type ($m_{T,X} = -^1/_2$, ax_2).). We note that while the $[AX]_2$ system is symmetrical with respect to J_{AA} and J_{XX}, this is not true for $[AX]_3$ systems. The A-spin spectra for $J_{AA} = 0$ and $J_{XX} \ll |J_{AX} - J_{AX'}|$ in $[A_nX]_3$ spin systems feature very distinct multiplets of five lines in addition to the singlet a_n sub-spectrum [25]. In addition, it can be noted that weakly coupled sub-spectra arise in the $[AX]_2$ system as long as $|J_{AX} - J_{AX'}| \gg |J_{AA}| + |J_{XX}|$ (see also Fig. S2). This is not sufficient in $[A_nX]_3$ spin systems, where J_{XX} must be negligible.

We now turn to the $[A_3X]_3$ system. In general, without simplifying assumptions about the values of the coupling constants, there are 9312 allowed A-transitions in this spin system out of which many hundreds can result in distinct lines [26]. Even with negligible J_{XX}, the spectrum is characterized by the presence of many lines, with wildly varying intensities (Fig. 2C). Under the simplifying conditions $J_{XX} \sim 0$ and $|J_{AX} - J_{AX'}| \gg |J_{AA}|$ the spectrum can now again be decomposed in simple sub-spectra. As there are three possible $m_{T,X}$-states for each side of the main J_{AX} doublet (e.g. $-^3/_2$, $-½$, $+½$ for the downfield triplet), there are again three sub-spectra. Recognizing that there are nine A-spins, the outer line is of the a_9-type. Since the spins within one A_3 group are magnetically equivalent, the center line becomes an a_6x_3 quartet, and the inner line is part of an a_3x_6 sub-spectrum, resulting in a septet (1:6:15:20:15:6:1) (Fig. 2D).

Similar reasoning can be used to show that $[A_2X]_2$ systems would have a_4 and a_2x_2 sub-spectra, and that spectra of $[A_2X]_3$ systems reduce to a_6, a_4x_2, and a_2x_4 sub-spectra. In short, we show here that in case of large $|J_{AX} - J_{AX'}|$ with respect to $J_{AA'}$ and negligible J_{XX}, the *a* and *b* species in sub-spectral analysis are in fact weakly coupled and the sub-spectra are simple multiplet patterns as in the case of weakly coupled spins.

4. Results

The focus of our study is a ^{13}C,^{15}N-labeled trimethyl amine, abbreviated as compound **1** (Fig. 3). While all methyl protons are chemically equivalent due to the molecular symmetry, the

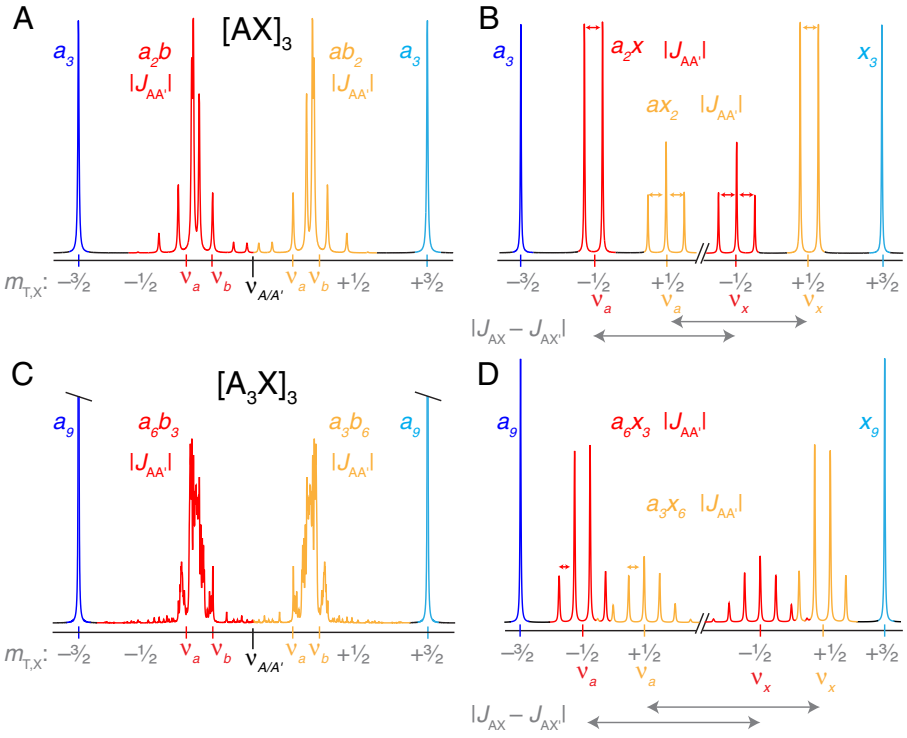

Fig. 2. Sub-spectral analysis of $[AX]_3$ and $[A_3X]_3$ spin systems when J_{XX} couplings are negligible. Simulated spectra of the A-part of the $[AX]_3$ (A,B) and the $[A_3X]_3$ spin system (C,D) spectrum using the following parameters: $J_{AX} = 10$, $J_{AX'} = 8$, $J_{AA'} = 2$, $J_{XX'} = 0$ Hz (A,C); in (B,D) J_{AX} is set to 150 Hz resulting in weakly coupled *ax*-type sub-spectra. In the $[AX]_3$ spin systems this results in a_2x and ax_2 sub-spectra, each composed of a doublet and a triplet. In the $[A_3X]_3$-spin system this results in a_6x_3 and a_3x_6 sub-spectra, each composed of a quartet and a septet. Total spin states of the X-spin is indicated for each sub-spectrum. Decomposition of the spectrum into sub-spectra is indicated (*a*-type in blue/cyan; *ab*/*ax*-type in red/orange). Effective Larmor frequencies of the virtual *a* and *b*(*x*) spins and their coupling constants are indicated. In (B,D) the Larmor frequency differences between the *a* and *x*-spin within one sub-spectrum is indicated. (For interpretation of the references to color in this figure legend, the reader is referred to the web version of this article.)

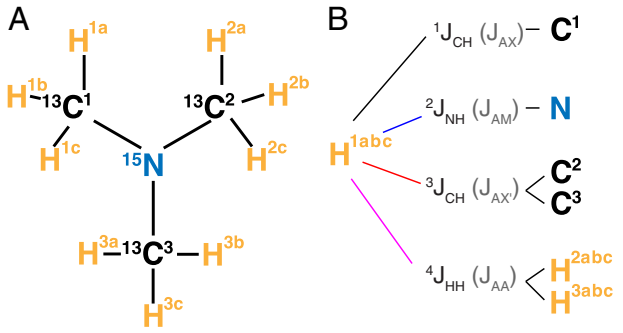

Fig. 3. Structure and spin topology of the amine group in the molecule studied. (A) The amine head group of 2-bromo-d_4-ethyl-^{13}C-trimethyl-^{15}N-ammonium is shown, featuring three geminal methyl groups. The deuterated bromo-ethyl group attached to the amine ^{15}N is omitted for clarity. Atoms are labeled with superscripts to allow their distinction in the main text. The full structure of the compound is shown in supplemental Fig. S1. (B) Scalar couplings experienced by the $H^{1a,b,c}$ spins, including to the geminal methyl groups H^2 and H^3. Corresponding AX nomenclature is shown between brackets. The coupling networks of the $H^{2a,b,c}$ and $H^{3a,b,c}$ spins can be found by permuting the atom labels. Protons in different methyl groups are magnetically inequivalent: protons in methyl group 1 have a large one-bond coupling ($^{1}J_{CH}$) to the directly attached C1 spin and much smaller three-bond coupling ($^{3}J_{CH}$) to C2, whereas protons in methyl groups 2 have three-bond couplings to C1 and a one-bond coupling to C2. Similar arguments can be made for all pairs of methyl groups, and for the ^{13}C spins.

introduction of ^{13}C-isotopes breaks their magnetic equivalence. This 13-spin system is thus best described as an $A_3A'_3A''_3MXX'X''$, or more compactly as a $[A_3X]_3M$ system, where A_3 represents the three ^{1}H spins in a methyl group, M is the ^{15}N spin, X is the ^{13}C carbon spin and the quotes are used to indicate magnetically inequivalent spins. As a result of the inequivalence, the proton 1D NMR spectrum of compound **1** can be expected to show splittings due to the four-bound coupling between the geminal methyl groups ($^{4}J_{HH}$) and the two-bond carbon-carbon coupling ($^{2}J_{CC}$).

As set out in the Theory section above, the appearance of AA′…XX′…–type spin systems depends strongly on the relative magnitudes of the coupling constants J_{AX}, $J_{AX'}$, J_{AA}, J_{XX}. In general, when all couplings are of comparable strength, the resulting spectrum will feature many lines with varying intensities, reflecting the strong coupling between magnetic inequivalent spin pairs. Moreover, the spectral complexity will increase rapidly with increasing size of the spin system, resulting in hundreds to thousands of distinct lines for an $[A_3X]_3$ spin system [26]. On the other hand, when some coupling constants dominate and others are negligible, the spectrum is greatly simplified. In particular, in case $J_{XX} \sim 0$ and $|J_{AX} - J_{AX'}| \gg |J_{AA}|$, the magnetic inequivalent nuclei become weakly coupled and the spectrum will reduce to a simple pattern of *ax*-type sub-spectra (see Theory section). In our case $|J_{AX} - J_{AX'}|$ corresponds to $|^{1}J_{CH} - {}^{3}J_{CH}|$, while J_{AA} and J_{XX} correspond $^{4}J_{HH}$ and $^{2}J_{CC}$ respectively. Thus, we may expect this simplifying condition to hold true for compound **1**, resulting in a spectrum similar to that in Fig. 2D.

4.1. Assignment of splittings in the ^{1}H spectrum

The proton 1D NMR spectrum of compound **1** is characterized by two highly asymmetric multiplet patterns separated by the large $^{1}J_{CH}$ (Fig. 4A). Ignoring the asymmetry, these patterns have the appearance of triplets, as expected considering the methyl protons are coupled to two ^{13}C spins by $^{3}J_{CH}$. Peak integration of the three triplet components shows the expected 1:2:1 ratio. As we will show below, the asymmetry is caused by unresolved $^{4}J_{HH}$ splittings.

The outer triplet component appears as a sharp doublet with 0.75 Hz splitting (Fig. 4B). This splitting is removed upon ^{15}N decoupling (Fig. 4C,D), proving that it is due to the $^{2}J_{HN}$ coupling interaction. This splitting is masked on the central and inner line of the triplet by their much broader appearance (Fig. 4B), but clearly present as can be inferred from the peak sharpening upon ^{15}N-decoupling (Fig. 4D).

The center and inner lines in the spectra of Fig. 4 show subtle signs of additional splittings. In an attempt to resolve these

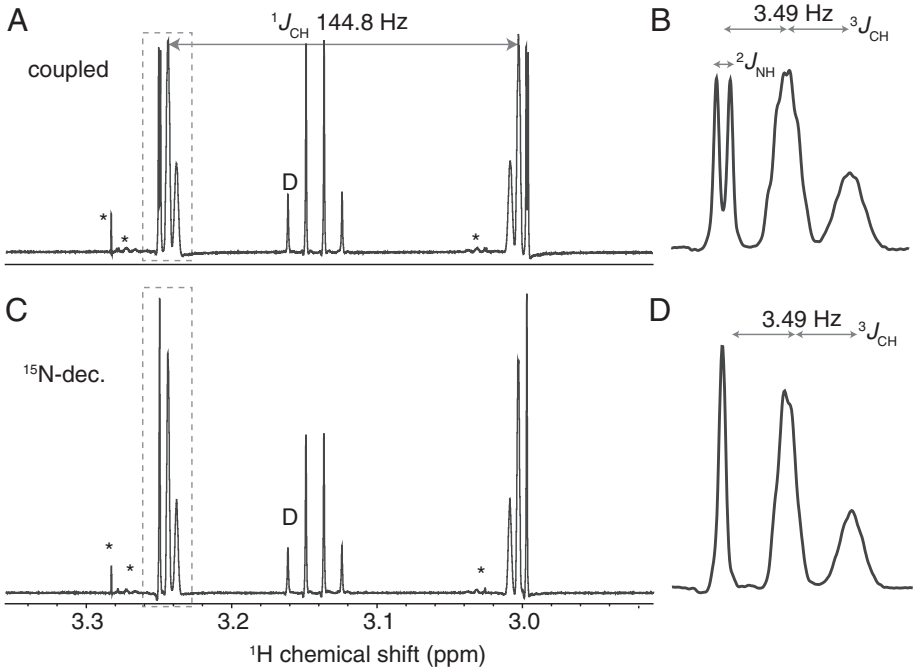

Fig. 4. Proton 1D NMR spectra of a ^{13}C/^{15}N-labeled trimethyl quaternary amine. Sections from the ^{1}H 1D NMR spectra without decoupling (A,B) and with ^{15}N decoupling (C,D) showing the signals from the nine chemically equivalent trimethyl protons. The boxed regions in (A,C) are expanded in (B,D) with indicated splittings in Hz. Signals from DIPEA (D) and minor impurities (*) are indicated.

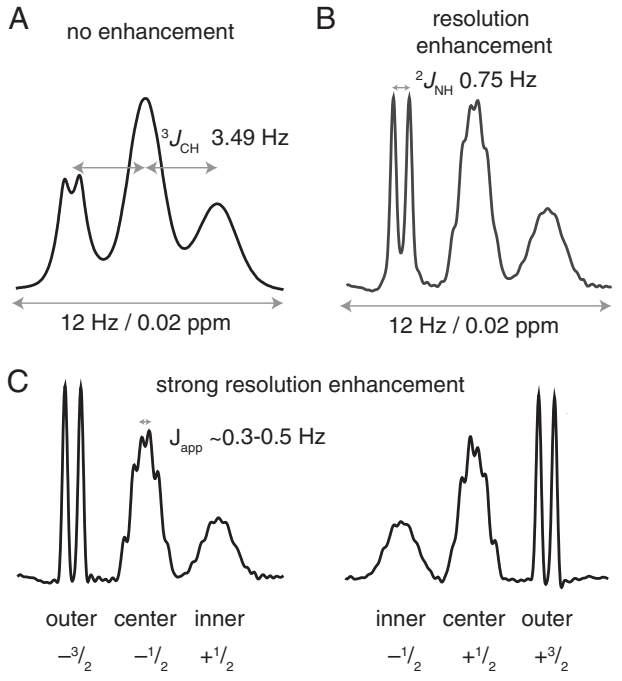

Fig. 5. Different fine structures are observed for each component of the $^3J_{CH}$ triplet. (A, B) show the downfield component of the main $^1J_{CH}$ doublet, (C) also shows the upfield $^1J_{CH}$ component. The different fine structure for each triplet component is already visible without any processing to enhance resolution (A), but more clear upon moderate (B) or strong (C), resolution enhancement through Lorentz-to-Gauss transformation. The additional splittings visible on the center and inner line are indicated in (C), together with the total spin state of the ^{13}C spins.

splittings, a high resolution spectrum was recorded with 8 s acquisition time and processed using different degrees of resolution enhancing Lorentz-to-Gauss transformations (Fig. 5). Without any window-function the spectrum shows a near perfect triplet, although the $^2J_{HN}$-splitting is only visible on the outer line (Fig. 5A). Processing with moderate or strong resolution enhancement uncovers small splittings on the center and inner lines only (Fig. 5B,C). This fine structure is different for the center and inner component, as is clear from their different shapes. This is consistently visible on both sides of the $^1J_{CH}$ doublet. The apparent coupling constant is on the order of 0.4 Hz, in line with *J*-coupling values expected for $^4J_{HH}$ or $^2J_{CC}$, and much smaller than $|^1J_{CH} - {}^3J_{CH}|$ (141.3 Hz). The increase in additional splittings going from the outer to center to the inner lines, i.e. there is a ^{13}C spin state dependent pattern of splittings, obeys the pattern shown in Fig. 2D fully.

4.2. Estimation of $^4J_{HH}$ and $^2J_{CC}$

We next applied the theory described above and decomposed the experimental spectrum into *ax*-type sub-spectra to extract an estimate for the $^4J_{HH}$ between the geminal methyl groups, thus assuming $^2J_{CC}$ is zero. Since compound **1** is an $[A_3X]_3M$ spin system, each line of the a_9, a_6x_3 and a_3x_6 sub-spectra in Fig. 2D will now be split into a doublet due to $^2J_{HN}$. The downfield component of the main $^1J_{CH}$ doublet was thus fitted as a sum of a doublet, a quartet of doublets and a septet of doublets. The resulting stick-plot and a simulated spectrum with the experimental lineshapes is shown in Fig. 6A,B. The best fit is obtained using 0.43 Hz for $|^4J_{HH}|$, and agrees very well with the experimental spectrum. An exact calculation of the ^1H spectrum of the $[A_3X]_3M$ system using the composite particle approach is shown in Fig. 6C, underscoring the validity of the weak coupling approximation. The numerical approach also allows evaluating the impact of non-zero values for $^2J_{CC}$ (Fig. 6C). Significant deviations from the experimental lineshape are already visible with very small non-zero values (0.4 Hz), most notably around the center of the inner multiplet. Furthermore, strong inequivalence effects are absent from the ^{13}C 1D spectrum (Fig. S3). Together, the exact simulations of both the ^1H and ^{13}C spectra strongly support a near-zero value for $^2J_{CC}$, at least $|^2J_{CC}| < 0.4$ Hz.

Notably, comparison of the experimental and numerically simulated spectrum highlights that the observed linewidths of the outer, center and inner line are unequal (Fig. 6A,C). There is a small, but significant, increase in linewidth going from the outer to the center and inner line. This effect has been accounted for in the fit

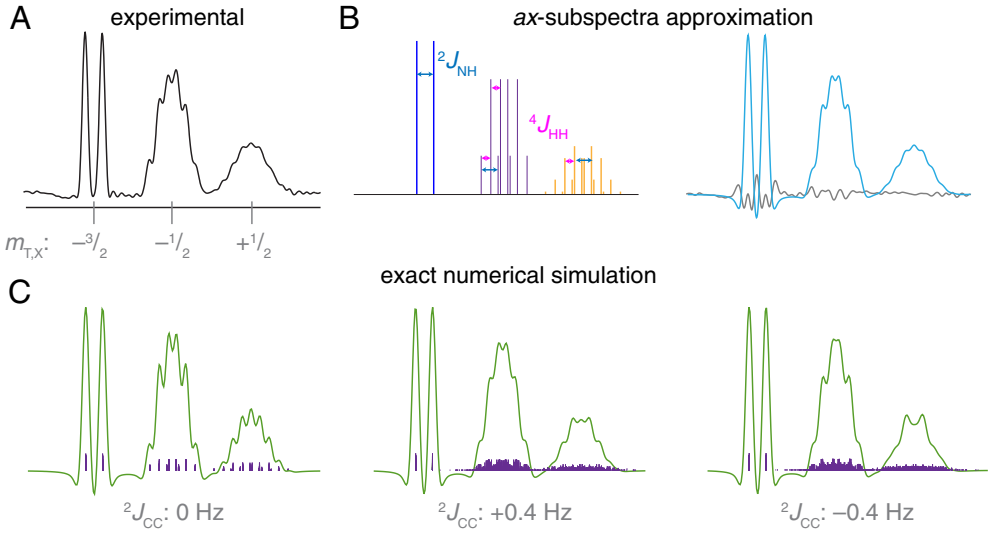

Fig. 6. Estimation of $^4J_{HH}$ and $^2J_{CC}$ in a quaternary trimethyl amine. (A) Downfield part of the experimental spectrum showing the $^1J_{CH}$-doublet. (B) Stick (left) and simulated spectrum (right) of using the weakly coupled *ax*-type sub-spectra approximation (see Materials and Methods for details) using $^1J_{CH} = 144.8$; $^3J_{CH} = 3.49$; $^2J_{NH} = 0.749$; $^4J_{HH} = 0.425$; $^2J_{CC} = 0$ Hz. The difference with the experimental spectrum is shown in gray on the right. In the stick spectrum, the $^2J_{NH}$ and $^4J_{HH}$ splitting are indicated for a number of lines. (C) Simulated spectrum using the composite-particle approach with the left spectrum using the *J*-values as in B as input, the middle and right spectrum have non-zero values for $^2J_{CC}$ as indicated. Stick-plot is shown as purple lines, overlaid with the summed spectrum in green. (For interpretation of the references to color in this figure legend, the reader is referred to the web version of this article.)

of Fig. 6B, where the center and inner lines are broadened by ~0.03 and 0.06 Hz, respectively, compared to the outer line.

4.3. Transformation to magnetic equivalence

The close agreement between the experimental spectrum and a fit based on a decomposition into *ax*-type sub-spectra suggests that the different methyl groups are in fact weakly coupled to each other due to $^4J_{HH}$. Phrased differently, the downfield center line and the upfield inner line form a weakly coupled *ax* spin system as do the downfield inner and upfield center line (cf. Fig. 2D). This effect can also be seen in the 2D DQF-COSY spectrum, which shows crosspeaks between the center and inner line (Fig. S4). Since spins *a* and *x* are weakly coupled and since there is a large frequency separation between them (cf. Fig. 2D), one may hypothesize the possibility to decouple their interaction. Indeed, a homo-decoupling experiment where the upfield component of the main $^1J_{CH}$ doublet, corresponding to the *x* spin species, are irradiated during acquisition results in the removal of all $^4J_{HH}$ splittings (Fig. 7A,B). The multiplets are collapsed to the expected triplet for a set of three fully equivalent methyl groups. Composite particle based calculation of this spin state-selective homo-decoupling experiment confirms the controlled transformation to a magnetically equivalent spin system (Fig. 7C). It is also of interest to note that the linewidths for each of the triplet components are very similar upon homo-decoupling.

5. Discussion

Magnetic inequivalent nuclei are regularly encountered in organic or inorganic compounds, where their presence can be used to infer molecular symmetry. Their NMR signals feature more lines and more intensities levels compared to a first-order coupling pattern, due to the strong coupling between magnetically inequivalent spin pairs. In this paper, we have presented an exceptional case of how magnetic inequivalence can affect the appearance of spectra, resulting in a sum of first-order coupling patterns. Compound **1**, an isotope-labeled trimethyl amine, presents an $[A_3X]_3M$ spin system where the coupling constants produce an extreme simplification of a spectrum that in typical cases would consist of hundreds to thousands of lines. We showed that this simplification depends on two conditions: (*i*) J_{XX} is near-zero; and (*ii*) $|J_{AX} - J_{AX'}| \gg |J_{AA}|$. We derived that under these conditions the spectrum can be decomposed into sub-spectra formed by fully equivalent spins (a_9-sub-spectra), and sub-spectra formed by weakly coupled *a* and *x* spins with coupling constant J_{AA} (a_6x_3/a_3x_6-sub-spectra).

We presented a stepwise analysis of $[AX]_2$, $[AX]_3$ and $[A_3X]_3$ spin systems, to understand and illustrate the salient features of the experimental spectrum, rather than a complete analytical description of the $[A_3X]_3M$ system. As noted by Diehl et al., the composite particle approach offers the most convenient route to solving the Hamiltonian [10]. In particular, this approach does not rely on molecular symmetry to factorize the Hamiltonian but rather factorizes based on spin states of the (composite) particles. In this description, the ^{1}H spectrum is described as a sum of 16 non-identical sub-spectra, where each sub-spectrum corresponds to one $m_{T,X}$ state and one particular combination of quartet and doublet spin states for the three methyl groups (see Fig. S5). Notably, all sub-spectra with the same $m_{T,X}$ value overlap and add up to the observed a_9, a_6x_3 or a_3x_6 patterns.

The overall spectrum can be reproduced using just 48 lines, thus classifying as a 'deceptively simple' spectrum where many transitions are (nearly) degenerate and/or have low transition probabilities [27]. This spectral simplicity made it possible to fit the experimental spectrum and extract a value of 0.43 Hz for the $^4J_{HH}$ between geminal methyl group in compound **1**. This is well in line with previous reports on geminal methyl coupling constants [28], in particular with a value of 0.41 Hz for the primary amine tert-butyl-amine [29]. Notably, direct measurement of $^4J_{HH}$ from the ^{13}C satellite peaks in an unlabeled compound failed since the presence of the quadrupolar ^{14}N nucleus induces ^{1}H line broadening through scalar relaxation of the second kind (data not shown). A near-zero value for the $^2J_{CC}$ matches the observation that these couplings are generally small in saturated aliphatic groups, and that they can be both positive and negative [30]. Notably, a reverse assignment of J_{HH} and J_{CC} is not possible since the A-spin spectrum of a $[A_3X]_3$ systems has different multiplet structures when $J_{AA} = 0$ [25].

When fitting the experimental lineshape with the weak coupling approximation, we found small but significant linewidth differences between the outer, center and inner line. This differential line broadening effect is removed in the homo-decoupled experiment, where the *x*-spins are decoupled from the *a*-spins. The observed broadening is thus most likely due to relaxation interference between the different ^{1}H-^{1}H dipolar interactions. A full analysis of this effect is beyond the scope of this paper.

The peculiar spectral manifestation of magnetic inequivalence in compound **1** may also be found in other compounds as long as the two limiting conditions are met. We thus expect that isotope labeled compounds with carbon/nitrogen-atoms separated by another hetero-nucleus such as C-O-C or C-S-C, or N-C-N type structures, as for instance ^{13}C-labeled dimethyl-ether, will show similar spectra with *ax*-type sub-spectra. The presence of the hetero-nucleus is required to make sure J_{XX} is negligible.

To the best of our knowledge this report is the first explicit analysis and experimental demonstration of a completely first-order spectrum for a magnetically inequivalent spin system. Other limiting cases resulting in spectral simplification have been described before, particularly in the work of Harris et al. [25,31–33]. In the

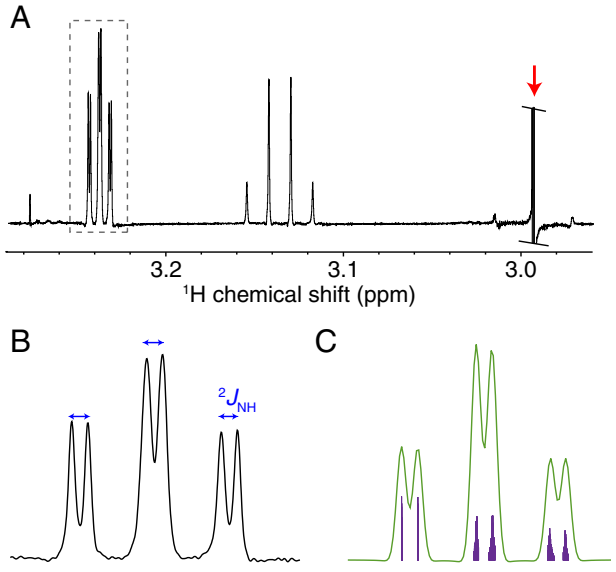

Fig. 7. Reduction to a fully equivalent spin system by spin state-selective homo-decoupling. (A) Experimental spectrum showing that the additional splittings on the center and inner lines of the downfield $^1J_{CH}$ component can be removed by selective homo-decoupling (~70 Hz/25 μW γB_2 CW irradiation) of the upfield component (indicated by the arrow). The boxed region is expanded in (B), showing a pure $^3J_{CH}$ triplet with each component split in a doublet due to $^2J_{NH}$. (C) Simulated spectrum using composite particle analysis. Spectrum was acquired and processed as those in Fig. 2. Stick-plot is shown as purple lines. (For interpretation of the references to color in this figure legend, the reader is referred to the web version of this article.)

case of $[PF_2]_2$-containing complexes, they showed that some sub-spectra may become first-order when one of the J_{PF} constants is very large [33]. Since in that case both J_{PP} and J_{FF} were non-zero, additional second-order sub-spectra remain. Another report on phosporous-fluorine complexes shows, without analysis, the ^{19}F spectrum of $Ni[PF_3]_4$ which is reminiscent of the spectrum of compound **1** [34]. Even though not all splittings can be resolved, it is clear that the spectrum deviates from the expected a_9x_3 quartet, suggesting that $^2J_{PP}$ is not negligible. The case described here stands out from such previous reports, as it presents an extreme simplification afforded by a 'perfect storm' of coupling constants.

Lastly, our work demonstrates a remarkable consequence of the weak coupling between the magnetically inequivalent nuclei: they can effectively be decoupled by spin state selective homo-decoupling. This transforms the spin system into a fully equivalent system, removing all $^4J_{HH}$ splittings from the multiplet. In our opinion, the spectrum of the ^{13}C-labeled trimethyl amine presented here is an extremely instructive illustration of the effects of magnetic inequivalence. Depending on your viewpoint the spectrum may be considered deceptively simple or deceptively complicated.

Acknowledgments

We thank Dr. Dennis Hetterscheid for discussions on group theory.

Funding: This work was supported by the Dutch Science Foundation NWO [NWO-CW VIDI 723.013.010 to HvI].

Appendix A. Supplementary material

Supplementary data associated with this article can be found, in the online version, at http://dx.doi.org/10.1016/j.jmr.2017.03.016.

References

[1] M. Karplus, Contact electron-spin coupling of nuclear magnetic moments, J. Chem. Phys. 30 (1959) 11–15, http://dx.doi.org/10.1063/1.1729860.
[2] H.S. Gutowsky, Chemical shifts and electron-coupled spin-spin interactions, Ann. N. Y. Acad. Sci. 70 (1958) 786–805, http://dx.doi.org/10.1111/j.1749-6632.1958.tb35431.x.
[3] H.M. McConnell, A.D. McLean, C.A. Reilly, Analysis of spin-spin multiplets in nuclear magnetic resonance spectra, J. Chem. Phys. 23 (1955) 1152, http://dx.doi.org/10.1063/1.1742204.
[4] E.B. Wilson Jr., Analysis of spin-spin interaction in the nuclear magnetic resonance spectra of symmetrical molecules, J. Chem. Phys. 27 (1957) 60–68, http://dx.doi.org/10.1063/1.1743719.
[5] J.A. Pople, W.G. Schneider, H.J. Bernstein, The analysis of nuclear magnetic resonance spectra: II. Two pairs of two equivalent nuclei, Can. J. Chem. 35 (1957) 1060–1072, http://dx.doi.org/10.1139/v57-143.
[6] F.S. Mortimer, The NMR spectrum of bicycloheptadiene, J. Mol. Spectrosc. 3 (1959) 528–535, http://dx.doi.org/10.1016/0022-2852(59)90045-1.
[7] P.L. Corio, The analysis of nuclear magnetic resonance spectra, Chem. Rev. 60 (1960) 363–429, http://dx.doi.org/10.1021/cr60206a003.
[8] P. Diehl, R.G. Jones, H.J. Bernstein, A simplified procedure for the analysis of complex nuclear magnetic resonance spectra: I. The principles of sub-spectral analysis, Can. J. Chem. 43 (1965) 81–93, http://dx.doi.org/10.1139/v65-011.
[9] R.G. Jones, R.C. Hirst, H.J. Bernstein, A simplified procedure for the analysis of complex nuclear magnetic resonance spectra: II. The analysis of symmetrical trifluorobenzene, the AA′A″XX′X″ system, Can. J. Chem. 43 (1965) 683–699, http://dx.doi.org/10.1139/v65-087.
[10] P. Diehl, R.K. Harris, R.G. Jones, Sub-spectral analysis, Prog. Nucl. Magn. Reson. Spectrosc. 3 (1967) 1–61, http://dx.doi.org/10.1016/0079-6565(67)80011-6.
[11] A. Connelly, R.K. Harris, D.J. Loomes, P.J. Beynon, Nuclear magnetic resonance spectral analysis for spin systems involving threefold symmetry. The spectrum of N(PF2)3, J. Chem. Soc., Faraday Trans. 2 (77) (1981) 915–928, http://dx.doi.org/10.1039/F29817700915.
[12] C.G. Barlow, D.L. Miller, R.A. Newmark, Complete analysis of the ^{31}P and ^{19}F NMR spectra of $[(PF_3)_3Mo(CO)_3]$, Magn. Reson. Chem. 38 (2000) 38–42, http://dx.doi.org/10.1002/(SICI)1097-458X(200001)38:1<38::AID-MRC546>3.0.CO;2-G.
[13] L. Kapička, D. Dastych, V. Richterová, M. Alberti, P. Kubáček, Analysis and calculation of the ^{31}P and ^{19}F NMR spectra of hexafluorocyclotriphosphazene, Magn. Reson. Chem. 43 (2005) 294–301, http://dx.doi.org/10.1002/mrc.1549.
[14] H.J. Reich, WINDNMR-Pro: Simulating NMR spectra with WINDNMR-Pro, 2002. <http://www.chem.wisc.edu/areas/reich/plt/windnmr.htm> (accessed February 28, 2017).
[15] H.J. Hogben, M. Krzystyniak, G.T.P. Charnock, P.J. Hore, I. Kuprov, Spinach–a software library for simulation of spin dynamics in large spin systems, J. Mag. Res. 208 (2011) 179–194, http://dx.doi.org/10.1016/j.jmr.2010.11.008.
[16] A.M. Castillo, L. Patiny, J. Wist, Fast and accurate algorithm for the simulation of NMR spectra of large spin systems, J. Mag. Res. 209 (2011) 123–130, http://dx.doi.org/10.1016/j.jmr.2010.12.008.
[17] J.W. Eaton, D. Bateman, S. Hauberg, GNU Octave version 3.0.1 manual: a high-level interactive language for numerical computations, CreateSpace Independent Publishing Platform, 2009. <http://www.gnu.org/software/octave/doc/interpreter>.
[18] J.S. Waugh, F.W. Dobbs, Strong coupling in nuclear resonance spectra. III. Systems containing many equivalent spins, J. Chem. Phys. 31 (1959) 1235–1239, http://dx.doi.org/10.1063/1.1730575.
[19] D.R. Whitman, L. Onsager, M. Saunders, H.E. Dubb, Proton magnetic resonance spectrum of propane, J. Chem. Phys. 32 (1960) 67–71, http://dx.doi.org/10.1063/1.1700949.
[20] G.W. Flynn, NMR spectrum of 1,1-difluoroethylene in the gas phase, J. Chem. Phys. 38 (1963) 226, http://dx.doi.org/10.1063/1.1733466.
[21] P. Diehl, Über eine Vereinfachung der Beschreibung und Analyse von komplizierten kernmagnetischen Resonanzspektren mit Hilfe von Teilspektren, Helv. Chim. Acta 48 (1965) 567–580, http://dx.doi.org/10.1002/hlca.19650480316.
[22] H.J. Bernstein, J.A. Pople, W.G. Schneider, The analysis of nuclear magnetic resonance spectra: I. Systems of two and three nuclei, Can. J. Chem. 35 (1957) 67–83, http://dx.doi.org/10.1139/v57-011.
[23] R.E. Richards, T. Schaefer, High resolution hydrogen resonance spectra of trisubstituted benzenes, Mol. Phys. 1 (1958) 331–342, http://dx.doi.org/10.1080/00268975800100411.
[24] C.W. Haigh, Notation for spin systems in nuclear magnetic resonance spectroscopy, J. Chem. Soc. A: Inorg. (1970) 1682–1683.
[25] E.G. Finer, R.K. Harris, Nuclear magnetic resonance spectra of the $[AX_n]_3$ spin system: calculations of X spectra when J_{xx}= 0, J. Chem. Soc. A: Inorg. (1969) 1972–1976, http://dx.doi.org/10.1039/J19690001972.
[26] J.F. Nixon, ^{19}F nuclear magnetic resonance spectra of some trisubstituted metal trifluorophosphine complexes. Examples of $[AX_3]_3$ nuclear spin systems, J. Fluorine Chem. 3 (1973) 179–185, http://dx.doi.org/10.1016/S0022-1139(00)84162-7.
[27] R.J. Abraham, H.J. Bernstein, The analysis of nuclear magnetic resonance spectra: V. The analysis of deceptively simple spectra, Can. J. Chem. 39 (1961) 216–230, http://dx.doi.org/10.1139/v61-025.
[28] W.J. Mijs, Long range spin spin coupling between protons of geminal methyl groups in 1,3-dioxane derivatives, Recl. Trav. Chim. Pays-Bas 86 (1967) 220–224, http://dx.doi.org/10.1002/recl.19670860213.
[29] D.J. Sardella, Substituent effects on long-range couplings in substituted propanes, J. Mol. Spectrosc. 31 (1969) 70–75, http://dx.doi.org/10.1016/0022-2852(69)90340-3.
[30] H.O. Kalinowski, S. Berger, S. Braun, 13C-NMR-Spektroskopie, Georg Thieme Verlag, Stuttgart, 1984.
[31] R.K. Harris, Comments on N.M.R. sepctra of the XnAA′Xn′ type, Can. J. Chem. 42 (1964) 2275–2281, http://dx.doi.org/10.1139/v64-334.
[32] E.G. Finer, R.K. Harris, M.R. Bond, R. Keat, Proton spectra of symmetrical cyclotriphosphazatrienes, J. Mol. Spectrosc. 33 (1970) 72–83, http://dx.doi.org/10.1016/0022-2852(70)90053-6.
[33] R.K. Harris, M.I.M. Wazeer, NMR spectra of the $[AX_2]_2$ and $[A[X]_2]_2$ types: the X transitions when |JAX| is large, as in the case of tetrafluorodiazadiphosphetidines, Ber. Bunsenges. Phys. Chem. 83 (1979) 697–702, http://dx.doi.org/10.1002/bbpc.19790830711.
[34] G.S. Reddy, R. Schmutzler, Phosphorus-fluorine chemistry. XVIII. Nuclear magnetic resonance studies on coordination compounds involving fluorine-containing phosphine ligands, Inorg. Chem. 6 (1967) 823–830, http://dx.doi.org/10.1021/ic50050a036.